

Upscaling European surface temperatures to North Atlantic circulation-pattern statistics

B. Orłowsky^a and K. Fraedrich^{b*}

^a Potsdam Institute for Climate Impact Research, P.O. Box 60 12 03, 14412 Potsdam, Germany

^b Institute for Meteorology, University of Hamburg, Bundesstraße 55, 20146 Hamburg, Germany

ABSTRACT: This paper examines reversal of the common downscaling path from large-scale circulation patterns to local surface weather: Can changes of near-surface temperature be used to predict changes in circulation-pattern statistics? A re-sampling (RS) scheme is applied, which generates ensembles of future series by assembling segments from past (or training) time series. The RS scheme is only constrained by known linear regression parameters of future annual mean temperatures. As circulation patterns, represented by the generalized patterns obtained by a cluster analysis, are part of the past series, the RS scheme also provides future time series of these patterns, conditioned only on the prescribed temperature evolution. In order to test whether changing statistics of temperature and circulation patterns are related to one another, a cross-validation experiment using global circulation model (GCM) data is conducted: Two independent 30-year periods are extracted from an Intergovernmental Panel on Climate Change (IPCC)-simulation (ECHAM5), the first of which serves as a training sample (2001–2030) for the RS scheme to simulate the temperature regime of the second (2071–2100). The estimates by the RS scheme and the GCM simulation for the second period are analysed with respect to circulation-pattern statistics. It is found that much of the changes from the first to the second period can be attributed to the temperature evolution. Future applications are discussed in the conclusions. Copyright © 2008 Royal Meteorological Society

KEY WORDS statistical upscaling; circulation pattern; climate simulation

Received 23 July 2007; Revised 25 January 2008; Accepted 16 June 2008

1. Introduction

A frequent task in climate research is downscaling of global circulation model (GCM) output, which is necessary whenever simulations of climate change need to be interpreted on a regional scale. While GCMs are suitable to estimate the global effects of, for example, future anthropogenic emissions on the climate of the earth (Solomon *et al.*, 2007, pages 755–790), their spatial resolution is too coarse to yield accurate estimates on the regional scale.

Transition from the global to the regional scale can be achieved by regional climate models that model physical processes as the GCMs do, however, on a finer spatial and temporal scale. The GCM output then defines the boundary conditions for these simulations (e.g. Kotlarski *et al.*, 2005). Other approaches to such a transition are based on statistical relationships between large-scale circulation patterns, which can be extracted from GCM runs, and local surface observations. They are especially useful for regions where much of the local variability is determined by the synoptic dynamics and sufficient observational data is available (see Zorita and von Storch, 1999, for an overview and Enke and Spekat, 1997, Timbal

and McAvaney, 2001, Beersma and Buishand, 2003, Diez *et al.*, 2005).

The common approach to exploit this relationship between circulation patterns and local weather, i.e. deducing local weather from circulation patterns, is reversed in this paper: Time series of circulation patterns over Europe and large parts of the North-Atlantic ocean are statistically simulated, conditioned only on near-surface temperature developments from the downstream continental part of this area [i.e. the re-sampling (RS-region, see Figure 1 and below)]. Circulation patterns are represented by generalized patterns obtained by a cluster analysis of daily 500 hPa fields. These experimental simulations try to answer whether the changes in statistics of larger scale circulation patterns can be attributed to changes of the downstream near-surface temperatures of a limited area. A necessary condition for such a statistical upscaling to be successful is that any potential statistical link between temperature and circulation patterns found during a training period, which implicitly constitutes the base of the statistically generated circulation-pattern series, is also valid for an independent future period.

The existence of such a link is relevant for a number of applications: (1) A check of whether simulations from different GCMs are able to reproduce this link may be useful to detect possible inconsistencies within the GCM representations of the underlying physical processes. (2) A distinction between different circulation patterns and

* Correspondence to: K. Fraedrich, Institute for Meteorology, University of Hamburg, Bundesstraße 55, 20146 Hamburg, Germany.
E-mail: klaus.fraedrich@zmaw.de

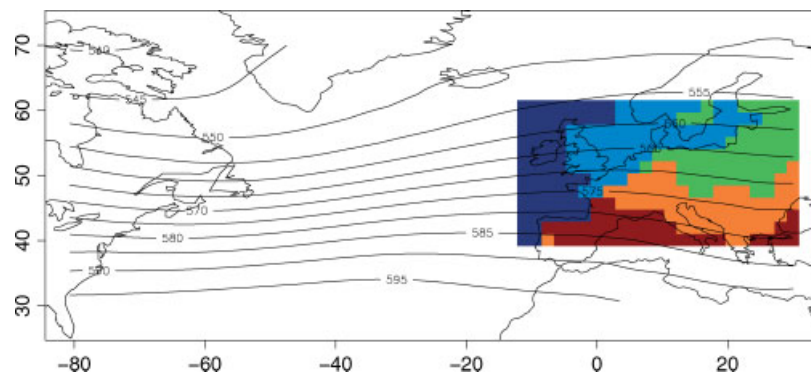


Figure 1. Mean 500 hPa heights from an IPCC-simulation by ECHAM5 for the training period 2001–2030 (contour lines in decameter). Temperatures from continental Europe (RS region) are used for the RS estimates. The subdivision of this region distinguishes different climate types (colour coded).

the strength of their individual links to near-surface air temperature may improve the physical understanding of the processes responsible for these relations, in particular, whether these relationships can change with changing climate. (3) Information on circulation-pattern statistics can be obtained by upscaling paleo- or historical time series of climate indicators such as tree rings (e.g. Briffa *et al.*, 1990) or reconstructed temperatures (e.g. Wang *et al.*, 1991; Mann *et al.*, 1998).

To assess whether such a link between near-surface air temperature and circulation patterns exists and can be used for upscaling, two independent 30-year periods from an exemplary GCM run, driven by an Intergovernmental Panel on Climate Change (IPCC)-scenario, serve as training and as future periods. Circulation-pattern series for the latter are statistically simulated, based on the statistical relationship between surface temperature and circulation patterns from the training period. These series are compared with the ‘true’ circulation-pattern series from the GCM data for the future period. Thereby, the success of this statistical upscaling and its underlying condition can be evaluated.

The paper is organized as follows: Section 2 introduces the RS scheme for the statistical simulations and describes the experimental set-up. In Section 3 the experiments are evaluated, followed by Section 4 summarizing and discussing the results. Appendix A and Appendix B provide more detailed descriptions of the RS scheme and the cluster analysis determining the circulation patterns.

2. Upscaling analysis: method and data

The RS scheme that generates ensembles of future time series was originally developed for regional climate simulations or scenarios using station data (Orlowsky *et al.*, 2008, based on Werner and Gerstengarbe, 1997). Here, it is applied to gridded surface data from a GCM run for a cross-validation experiment.

2.1. Re-sampling (RS) scheme

One of the most important properties of the RS-scheme is that the only constraints it uses are the two parameters

of a regression line, which the series of annual means of a characteristic climate variable has to correspond to. In this paper, this characteristic variable is the near-surface air temperature.

The underlying assumption of the RS scheme is that sequences of observations and of observed fields from the training period can occur again or occur in a very similar manner in the future period. Hence, it assembles future series from segments of the observed time series in terms of an analogue search (e.g. Lorenz, 1969, Fraedrich and Rückert, 1998, Zorita and von Storch, 1999). No trend is removed from the training data. Thereby, physical consistency of both the spatial fields and the combinations of different variables is guaranteed for time series simulated by the RS scheme. A set of heuristic rules ensures that the RS-scheme series, besides complying with the prescribed regression parameters, exhibit realistic annual cycles and persistence. Stochastic elements in the approach enable the generation of simulation ensembles.

Generating a future series can thus be seen as defining a date-to-date mapping, by which each date of the future period is assigned a date of the training period. Since an observed circulation pattern is attached to each surface observation date, the RS scheme provides future series not only of surface data but also of circulation patterns. See Appendix A for an introductory description of the steps which generate the RS-scheme series, explained in more detail in (Orlowsky *et al.*, 2008).

2.2. Data and experimental set-up

For this study, two periods with different temperature regimes are extracted from an exemplary GCM run: the first period serves as training period, the second one as ‘future’ period. Prescribing only the linear evolution of the future near-surface air temperature, the time series for the future period (i.e. the date-to-date mapping by the RS scheme) can be constructed utilizing the temperature data from the training period (see below). Future time series of circulation patterns can be estimated by the RS scheme and thus be compared with the ‘true’ future series obtained by the GCM simulation. This gives insight into whether changes in statistics of circulation patterns can be attributed to the evolution of surface temperatures.

All data used for this experiment are retrieved from IPCC simulations by a coupled atmosphere–ocean GCM (ECHAM5/MPI-OM, (Roeckner *et al.*, 2003; Marsland *et al.*, 2003; Roeckner, 2006) for the years 2001–2100. It is driven by the IPCC-A1B-scenario (Nakicenovic and Swart, 2001, Chapter 5) for 2001–2100. The simulation is run on a T63-grid, corresponding to a horizontal extension of the grid cells of about 200 km.

Two time slices of 30-year lengths are extracted to obtain a training period (2001–2030) and a future period (2071–2100). The two periods differ strongly with respect to their temperatures: averages over all grid cells in the RS region (Figure 1) give 10.33 °C for the training and 13.05 °C for the future period. If changes in circulation pattern statistics can be linked to surface air temperature at all, these links would become apparent in such a setting.

2.3. Climatological setting: circulation patterns and near-surface air temperature

Circulation patterns are identified from daily 500-hPa height fields by means of a cluster analysis. As much of

central European weather is governed by synoptic activity over the North-Atlantic, the area selected for identifying the circulation patterns extends from 80°W to 30°E and from 30°N to 70°N (Figure 1).

From the daily 500-hPa fields of the training period, circulation patterns are identified by standard cluster analysis (Appendix B). Since the focus is on the atmospheric states rather than on their anomalies, no annual cycle was eliminated, as e.g. in (Kageyama *et al.*, 1999). The circulation patterns are characterized by the centroids obtained from a cluster analysis, and their number is set to three. Thus assigning each field one of three possible states implies a strong reduction of the information in the original data. This loss of information is compensated by a gain of an interpretability of the patterns.

In the left column of Figure 2, the three patterns used for this study are shown as anomalies from the mean geopotential height field (which is plotted in Figure 1). The right column gives the monthly distributions of the respective patterns, both for the training and the future periods.

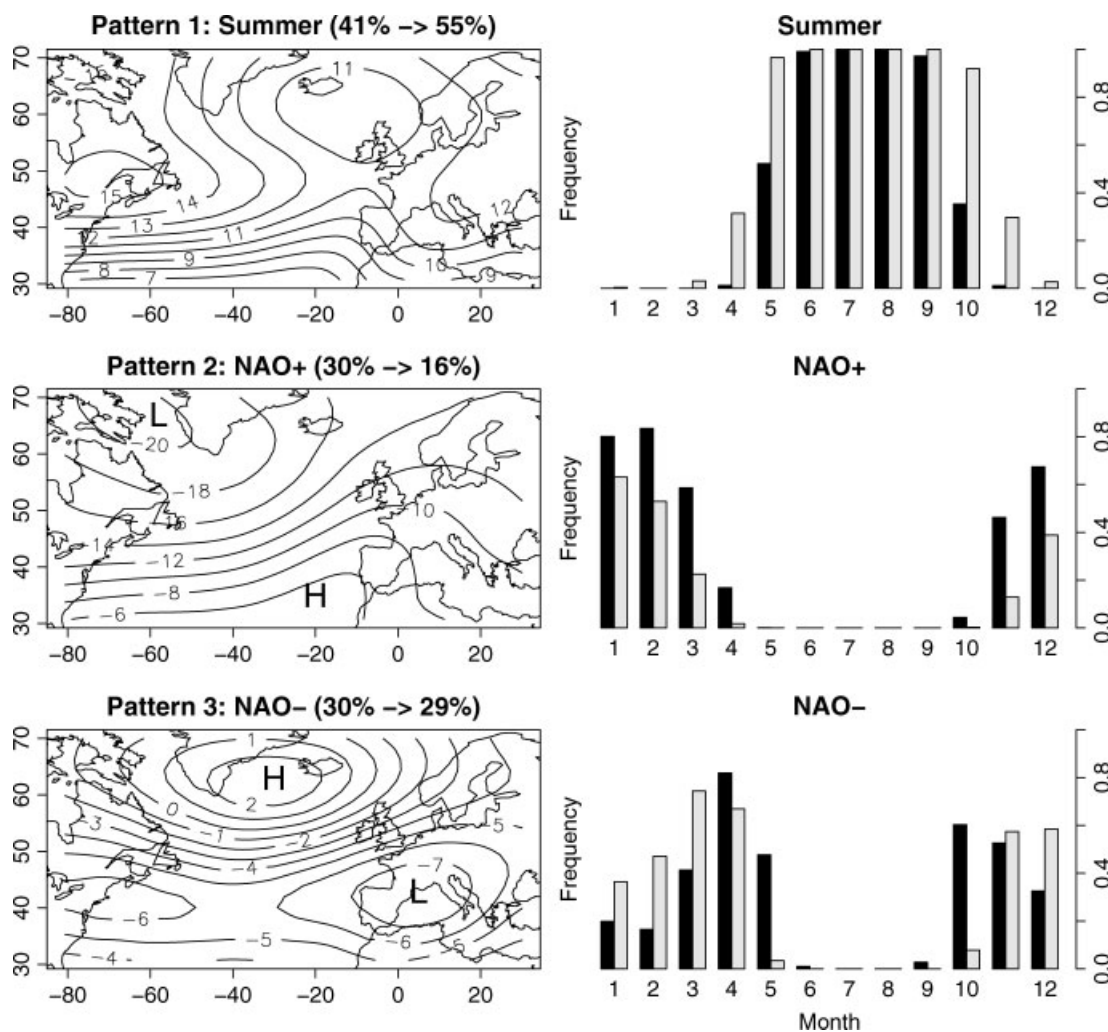


Figure 2. Three circulation patterns and their relative frequencies from training to future period (in %) extracted from the 500 hPa heights of the training period (left, contours in decametre), plotted as anomalies from the mean pattern (see Figure 1). Monthly relative frequencies of the three pattern occupations are on the right for the training period (black) and the future period (grey). Frequencies are normalized to 1 for each month.

1. Pattern 1 is referred to as the *summer* pattern, as it occurs mainly in this season. Adding the mean (Figure 1) to the anomalies, it is characterized by zonal isobars of relatively high values and a flat meridional gradient.
2. Pattern 2 corresponds to the positive phase of *NAO+* with a pronounced low over the North-western Atlantic and a high over the Azores, which occurs mainly during the winter season.
3. Pattern 3 is referred to as *NAO-*. It consists of the reversed *NAO+* dipole with a high close to Iceland and a low over the Mediterranean. It occurs mainly in spring and autumn and less frequently in winter.

Experiments with differing cluster numbers do not yield qualitatively different results (not shown). An increasing number of clusters mainly leads to further differentiation of the winter season, as variability is much larger in winter than in summer. Concentrating on the main modes of winter variability (*NAO+* and *NAO-*), we keep three clusters in the analysis.

The *NAO+* (*NAO-*) pattern is tested by principal component analysis (PCA, e.g. Jolliffe, 1990) of the 500-hPa heights. This PCA yields a time series for the *NAO+* pattern. The days at which this *NAO* series is at least 2 standard deviations higher (lower) than its mean, the *NAO+* (*NAO-*) days, are compared with the days of Pattern 2 (Pattern 3) in Table 1. It shows the respective contingency tables that underline the interpretation of Pattern 2 (Pattern 3) as *NAO+* (*NAO-*). See (Wanner *et al.*, 2001) for a review of *NAO*. The *NAO+* and *NAO-* patterns are similar to those found by (Cassou *et al.*, 2004), although the exact orientation of the *NAO* dipole differs (their patterns are found by cluster analysis of monthly winter means of sea-level pressure data from National Centers for Environmental Prediction (NCEP) reanalysis).

Since the summer pattern is the only pattern during the summer season, no transitions to different ones occur (see monthly distributions in Figure 2). Only in spring and autumn, the summer pattern can be replaced by one of the *NAO* patterns. Winter half-years are more varied, as *NAO+* and *NAO-* coexist.

The circulation-pattern series for the future period is determined by assigning each of the future (2071–2100) daily 500-hPa fields to the circulation pattern to which it is most similar. Differences between training and future circulation-pattern statistics are discussed in the following Section 3.

Table I. Contingency tables of *NAO+* (*NAO-*) and its corresponding circulation Pattern 2 (Pattern 3). Numbers in (%), normalised row-wise.

| | Pat. 2 | | Pat. 3 | |
|-----------------|------------|--------|------------|--------|
| | not Pat. 2 | Pat. 2 | not Pat. 3 | Pat. 3 |
| <i>NAO+</i> | 80 | 20 | 81 | 19 |
| not <i>NAO+</i> | 29 | 71 | 28 | 72 |

Table II. Temperature regime of the future period from the GCM data and its reproduction by the RS ensemble.

| Region | T_{mean} (°C) | | Lin. Trend (K) | |
|--------------------|------------------------|-----------|----------------|---------|
| | GCM | RS | GCM | RS |
| 1 Atlantic | 13.9 | 13.8–14.0 | 0.5 | 0.4–0.6 |
| 2 Coastal cool | 10.9 | 10.7–11.1 | 1.2 | 1.0–1.4 |
| 3 Coastal warm | 17.7 | 17.5–17.9 | 1.2 | 1.0–1.4 |
| 4 Continental cool | 10.2 | 9.8–10.5 | 1.3 | 1.0–1.7 |
| 5 Continental warm | 14.2 | 13.9–14.6 | 1.4 | 1.1–1.7 |

Near-surface air temperatures from the RS region (12°W–30°E, 40°N–60°N, see Figure 1) are used as a base for the RS estimates. The RS region is further divided by cluster analysis (Appendix B) into five sub-regions: an Atlantic part of the region (dark blue), a warm (brown) and a cold (light blue) type of coastal climate, and two types of rather continental climate – a warmer one (orange) and a cooler one (light green).

The conditioning surface weather variables for the RS estimates are the average temperature series of these sub-regions, which enter the RS scheme in two ways (Appendix A): (1) The future series are assembled from segments of the training series. These segments are characterized by their temperatures from the training period. (2) The future series are assembled such that they represent the temperature regime of the future period, prescribed by the linear temperature evolution during the future period. That is, the two parameters of a regression line, which are estimated from the future annual mean temperatures of each sub-region, are prescribed to the RS scheme. See Table 2 for the temperature regime of the future period in the GCM data and its reproduction by the RS scheme. Hence, the selection of the segments from the training series for assembling the future series is based on the temperatures from the training period, and the boundary conditions for the RS estimates are prescribed by the linear future-period temperature trends.

A single RS-simulation (Section 2, Appendix A) is only one realization from possible RS-simulations compatible to the prescribed regression parameters and the set of heuristic rules. To estimate its range, an ensemble of 100 simulations is generated for this experiment and evaluated in terms of circulation-pattern statistics.

3. Upscaled circulation patterns: training and future-period statistics

A first impression of the link between circulation patterns and near-surface air temperatures in the GCM and RS-scheme simulations is given by the correlation maps in Figure 3, for which the explained variance of a linear model is calculated, which links the 500-hPa series of each grid cell with the five averaged temperature series

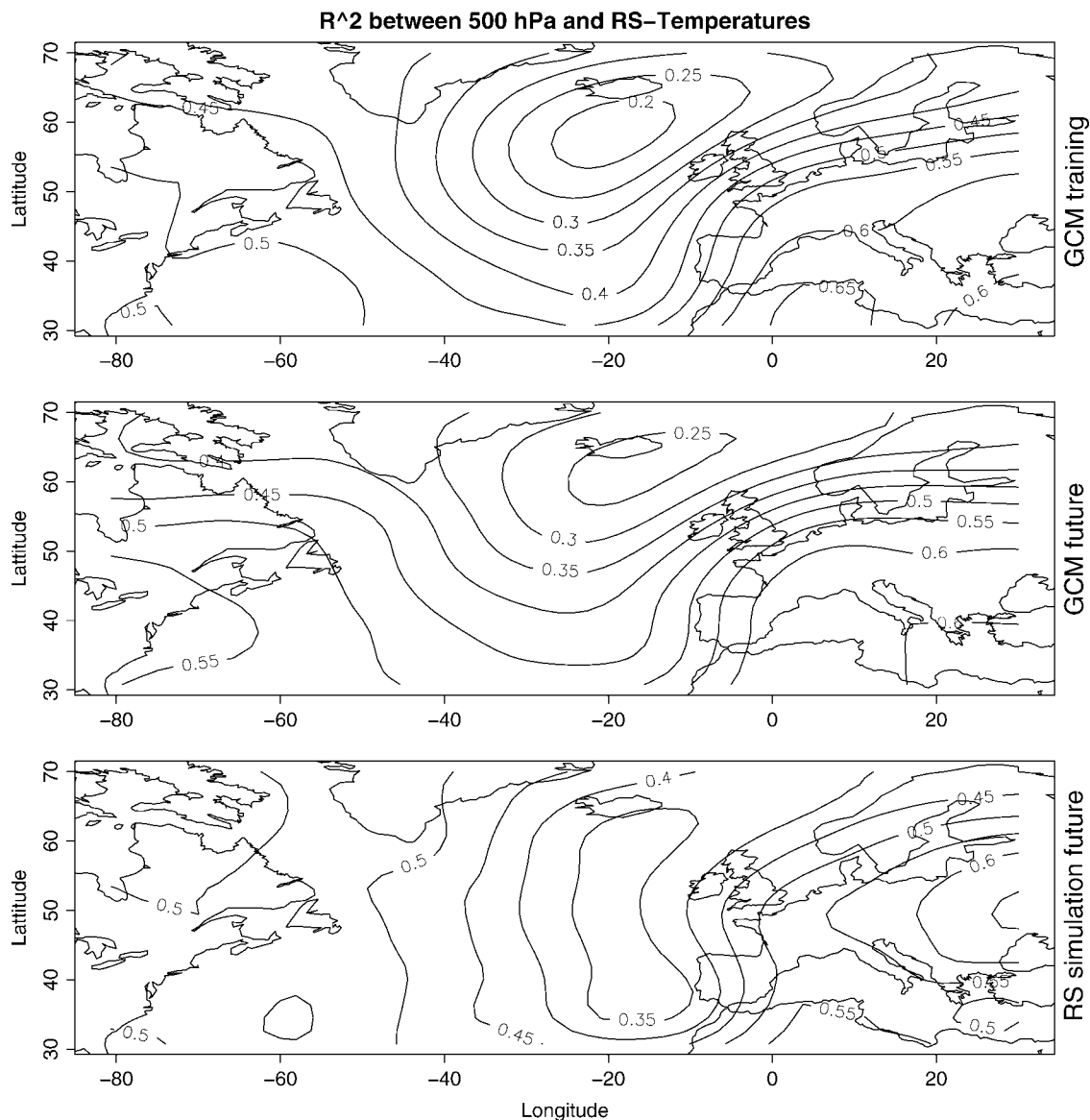


Figure 3. Explained variance R^2 for the 500-hPa series of each grid cell, modelled by linear regression on the five averaged temperature series from the sub-regions of the RS region (see Figure 1 and Section 2.3). Top: GCM, training period (2001–2030); middle: GCM, future period (2071–2100); bottom: an arbitrarily chosen simulation of the future period from the RS ensemble.

of the continental downstream RS-area (Section 2.3),

$$G_{ij}(t) = \alpha + \sum_{k=1}^5 \beta_k T_k(t) + \epsilon(t)$$

$G_{ij}(t)$ denotes the time series of the geopotential 500-hPa heights in grid cell ij and $T_k(t)$ represents the averaged time series from sub-region k with $k = 1 - 5$ (Table 2). Coefficients α and β_k with $k = 1 - 5$ are estimated by linear least-square regression, assuming independent and Gaussian residuals $\epsilon(t)$.

The maps from the GCM data show a rather strong positive correlation for both periods over the continental parts of the area, in particular over Europe, while this correlation is much weaker over the central Atlantic part, i.e. the region of the NAO-activity (Section 2.3). This

hints at limited feasibility of the proposed upscaling by simple linear correlation models.

The bottom map in Figure 3 shows the spatial correlation pattern estimated from an RS-scheme simulation of the future period chosen at random from the ensemble. The RS correlation pattern apparently differs from the GCM pattern; however, the general features of the GCM data – high correlation over the continental parts, low correlation in the NAO-region – are reproduced.

The following are some essential statistics with respect to the generalized circulation patterns (Section 2.3), which are analysed and compared for the RS and GCM simulations of the future period. The analysed statistics are (1) frequencies of occupation, (2) transition frequencies, and (3) period length distributions of the generalized circulation patterns. This analysis provides more detailed

information on the persistence of the correlation features and whether they can be reproduced by statistical upscaling.

Occupations: Table 3 shows how frequently the circulation patterns (summer, NAO+, NAO−) are visited in the training and the future GCM simulations (first line) compared with the future RS estimates (second line). The following results are noted:

- (1) The range of future frequencies estimated by the RS scheme for the summer pattern is narrow and agrees remarkably with the GCM frequency for the future period, which is considerably higher than for the training period.
- (2) The occupation frequency of the NAO+ pattern drops significantly from the training period to the future period in the GCM data. This however must not be confused with a weakening of the NAO+ in the GCM simulation: the NAO+ time series from the PCA does not exhibit a decreasing trend (not shown). Rather, together with the rising temperatures the overall 500-hPa heights increase (from 568 dm for the training period to 574 dm for the future period), and NAO+ states are more frequently assigned as summer pattern (with its overall higher level) during the future than during the training period. In the RS-scheme ensemble, NAO+ pattern frequencies are also lower than the one in the training period, but the decrease is not fully captured.
- (3) For the NAO− pattern, frequencies hardly change from training to future period in the GCM data. They are a little underestimated by the RS-scheme ensemble.
- (4) The ratio between NAO+ and NAO− occupations is approximately the same for the future RS estimates and the GCM training data, in contrast to the strong decrease of NAO+ occupations in the GCM data from training to future period. While the GCM simulates different NAO dynamics for the two periods, the RS estimates are conservative with respect to NAO pattern statistics.

It is interesting to see that in the future GCM simulation, the summer pattern becomes more frequent: the warming from the training to the future period is produced by a natural extension of the summer season. The

Table III. Occupation frequencies of the circulation patterns. First row gives the frequencies from the GCM data for the training and the future period (bold). Second row contains the range of the RS-scheme ensemble estimates of the future frequencies.

| Circulation pattern | Summer | NAO+ | NAO− |
|---------------------------|--------------------|--------------------|--------------------|
| GCM: training → future | 0.41 → 0.55 | 0.30 → 0.16 | 0.30 → 0.29 |
| RS ensemble: future range | 0.54–0.56 | 0.20–0.24 | 0.21–0.25 |

close agreement between the RS-scheme ensemble estimates and the ‘true’ occupation frequency supports this interpretation: The RS scheme generates time series for a climate warmer than the training climate, for which the warmer (summer) segments of the training series have to be preferentially selected. That is, for occupation frequency, the link between surface temperature and circulation patterns of the training period also holds for the future period. For the winter half year and the NAO+ and NAO− patterns, GCM simulation and RS estimates differ for the future period. Since the RS scheme conserves the link between circulation patterns and downstream continental near-surface temperatures from the training period, this hints at a changing relation between NAO+ (NAO−) and downstream near-surface temperatures in the GCM simulation.

Transitions: Table 4 shows the relative transition frequencies of all possible pairs of circulation-pattern successions for the training and the future periods from the GCM data (first row of each pattern). Some transitions differ strongly between the two periods. This is especially evident for the persistencies of the circulation patterns, which are located diagonally in the table. The second row of each circulation pattern in Table 4 indicates the range of the transition frequencies as estimated by the RS scheme for the future period.

For the ‘mixed’ (off-diagonal) transitions, there is a close agreement between the RS-estimated frequencies and the ‘true’ ones of the future period. For the persistence transitions, the picture is more diverse:

- (1) For the summer-pattern persistence, the increase of the transition probability from training to future period is well reproduced by the RS scheme.
- (2) A notable difference occurs for the NAO+ persistence, which is overestimated by the RS scheme, in agreement with the overestimation of the occupation frequency of this pattern (Table 3). However, since these persistence transitions of the RS-scheme ensemble are much closer to the ‘true’ one of the future period than to that of the training period, the RS scheme still captures the tendency of the evolution from training to future period correctly.
- (3) The NAO− persistence transition is underestimated, in accordance with the underestimation of the respective frequency (Table 3).
- (4) As for the occupation frequencies, the ratio between NAO+ and NAO− persistencies of the training period is conserved by the RS ensemble for the future period (the respective persistencies in the GCM simulations differ significantly for NAO+).

Since the summer pattern entirely dominates the summer season, no transition frequency changes are possible in summer. Therefore, considerable increase of the summer persistence takes place only at onset and offset of summer: summer in terms of circulation patterns begins earlier and lasts longer, affirming the interpretation of the occupation analysis that the warming from the training to

Table IV. Transition frequencies of the circulation patterns. The first row of each pattern gives the frequencies from the GCM data for the training and the future period (bold). The second row of each pattern contains the range of the RS ensemble estimates of the future transition frequencies.

| Circulation pattern | | Summer | NAO+ | NAO– |
|---------------------|-------------|--------------------|--------------------|--------------------|
| Summer | GCM | 0.40 → 0.54 | 0.00 → 0.00 | 0.01 → 0.01 |
| | RS ensemble | 0.52–0.54 | 0.00–0.00 | 0.01–0.02 |
| NAO+ | GCM | 0.00 → 0.00 | 0.27 → 0.14 | 0.02 → 0.02 |
| | RS ensemble | 0.00–0.00 | 0.17–0.21 | 0.02–0.03 |
| NAO– | GCM | 0.01 → 0.01 | 0.02 → 0.02 | 0.26 → 0.26 |
| | RS ensemble | 0.01–0.02 | 0.02–0.03 | 0.16–0.21 |

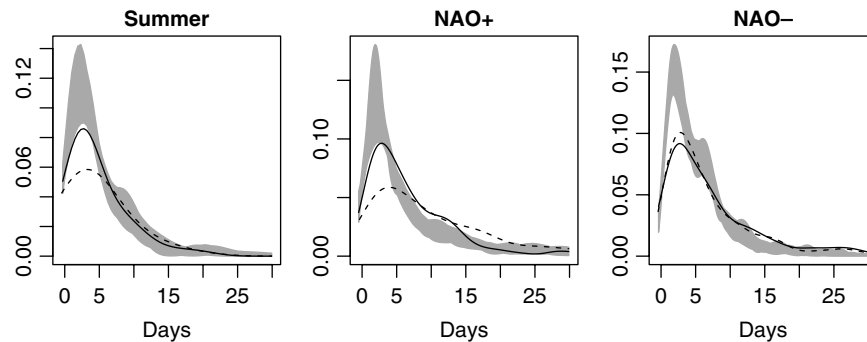


Figure 4. Distributions of the circulation-pattern period lengths (in days): GCM simulations of the training period (dashed) and the future period (solid), range of the RS ensemble estimates of the future distributions (shaded).

the future period is essentially produced by an extension of the summer season (see also Figure 2).

Note that the probabilities of transition (Table 4), if rescaled to a transition probability matrix, can be used as a first order Markov chain predicting circulation patterns.

Period lengths: The probability densities of the individual circulation-pattern period lengths are a measure of persistence and estimated by applying a Gaussian kernel with a bandwidth according to (Sheather and Jones, 1991). Estimated densities are shown in Figure 4, black solid lines for the GCM circulation patterns of the future period, and dashed lines for the training period. The grey shaded area gives the range of the RS-scheme ensemble.

The distributions for the summer and the NAO+ pattern reveal a tendency towards shorter period lengths for the future period. The RS-scheme ensemble shows this tendency as well, with short period lengths being much favoured. As for occupation and transitions, period lengths of the NAO– pattern do not change from training to future period in the GCM data, but for the RS ensemble estimates, they are clearly skewed towards short period lengths.

4. Discussion and conclusions

This article attempts to answer the following questions: Is there a link between the evolution of surface temperatures in a limited region (such as central Europe) and potential changes in circulation patterns dominating its climate? Can such a link be used to predict changing circulation-pattern statistics from changes of temperature alone, i.e.

is it possible to obtain circulation patterns by merely upscaling temperatures?

Two 30-year periods are extracted from a GCM run, which differ significantly with respect to surface air temperature and circulation pattern statistics. For upscaling to be possible, statistical relations between temperature and circulation patterns from the first (training) period must also hold for the second (future) period. Three circulation patterns are taken into account: a summer pattern dominating the summer season and two patterns corresponding to the positive and negative phase of NAO, respectively.

An resampling (RS) scheme is employed, which is originally designed to generate ensembles of future (or scenario) surface weather time series from past observations by rearrangement rules. The RS scheme is implicitly based on the time evolution properties of the observed time series and constrained only by a prescribed linear temperature change for the future period. Since future series are assembled from segments of observed time series (and circulation patterns are part of the latter), they also generate future series of circulation patterns that are conditioned on near-surface temperatures and on the time statistics of the training period. If the circulation-pattern statistics estimated by the RS scheme ensemble are similar to the GCM statistics of the future period, the temperature and circulation relation in the training period also hold for the future period.

This comparison is based on statistics characterizing circulation pattern dynamics: their occupation, transition, and period length frequencies. Despite the climatological differences between training and future periods, the

RS scheme is able to largely reproduce the GCM- simulated circulation-pattern statistics. This holds for the summer circulation pattern, of which the frequency increases strongly in the course of the rising temperatures: warming is produced by an extension of the summer season, well represented in the RS ensemble. That is, the statistical links between temperature and the summer pattern of the training period remain for the future period. For the NAO+ pattern, the statistics in the GCM simulation change from training to future period, with occupation frequency decreasing. In contrast, the RS ensemble estimates are conservative with respect to the pattern-temperature relation of NAO+ and NAO-: future estimates and training periods exhibit very similar statistical relations between NAO+ and NAO-. While the summer pattern in future GCM simulation and the related RS estimates agree on larger summer pattern occupations to produce the required warming, the winter variability (dominated by NAO+ and NAO-) changes in the GCM simulation (reduced NAO+, constant NAO-), in contrast to the unchanged RS estimates of occupations and transitions, i.e. the RS scheme conserves the statistical links between circulation patterns and near-surface temperature of the training data, the discrepancy between GCM simulation and RS estimates for the future period mean, that the link between NAO+ (NAO-) and the conditioning near-surface temperature changes in the GCM simulation. This may be due to changing land-/sea-surface temperature contrasts which are not taken into account by the regional RS scheme for continental Europe.

Further applications are envisaged: (1) Testing GCM simulations and their representation of the statistical circulation properties: possible inconsistencies in simulations may be uncovered by employing the RS scheme and the experimental set-up as a cross-validation tool. (2) Analysing the physics of circulation pattern links to near-surface air temperature in order to understand the

interplay between large-scale circulation and local surface weather. (3) Upscaling applied to paleo- or historical time series: the RS scheme may be employed at different time scales (monthly or seasonal) to obtain information about circulation-pattern statistics of the past. This can be achieved by upscaling historical climate indicators such as tree rings or reconstructed temperatures, using the present day climate as training data.

Acknowledgements

The authors are deeply indebted to F.-W. Gerstengarbe for his most helpful comments on early versions of this manuscript, and to Oliver Bothe for his assistance with the ECHAM5-data. Support by Sonderforschungsbereich SFB 512 is gratefully acknowledged. The authors are very grateful to an anonymous reviewer for his convincing comments and suggestions during the revision process.

Appendix A

The RS-scheme future series are assembled from segments of the observed series: the approach generates a mapping from dates of a future period to dates of the training period. As mentioned in the introduction, this mapping is constructed such that the corresponding series yield annual temperature means which feature a prescribed regression line. See Figure 5 for an illustration of this setting.

Here, only the outline of this construction can be given. For a detailed description, the reader is referred to (Orlowsky *et al.*, 2008).

Single location: If only a series for a specific location is needed, e.g. a meteorological station or a single grid cell, no spatial dependencies have to be taken into account. Figure 6 summarizes the generation of the date-to-date

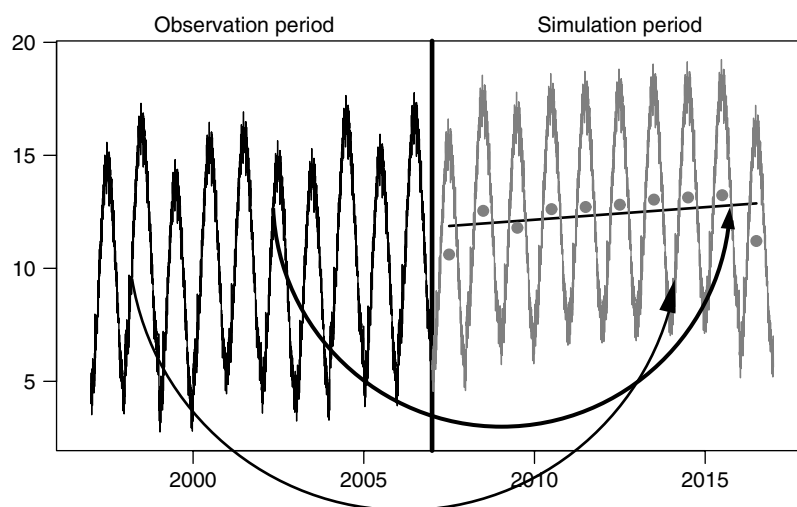


Figure 5. Assembling future series from segments of observed series, corresponding to a prescribed regression line. Illustrative temperature series from the training period and the prescribed regression line for the future period (black); (in grey) future temperatures of which the annual means (grey dots) feature the prescribed regression line. This series is assembled from elements of the observation series, as illustrated by the two exemplary arrows.

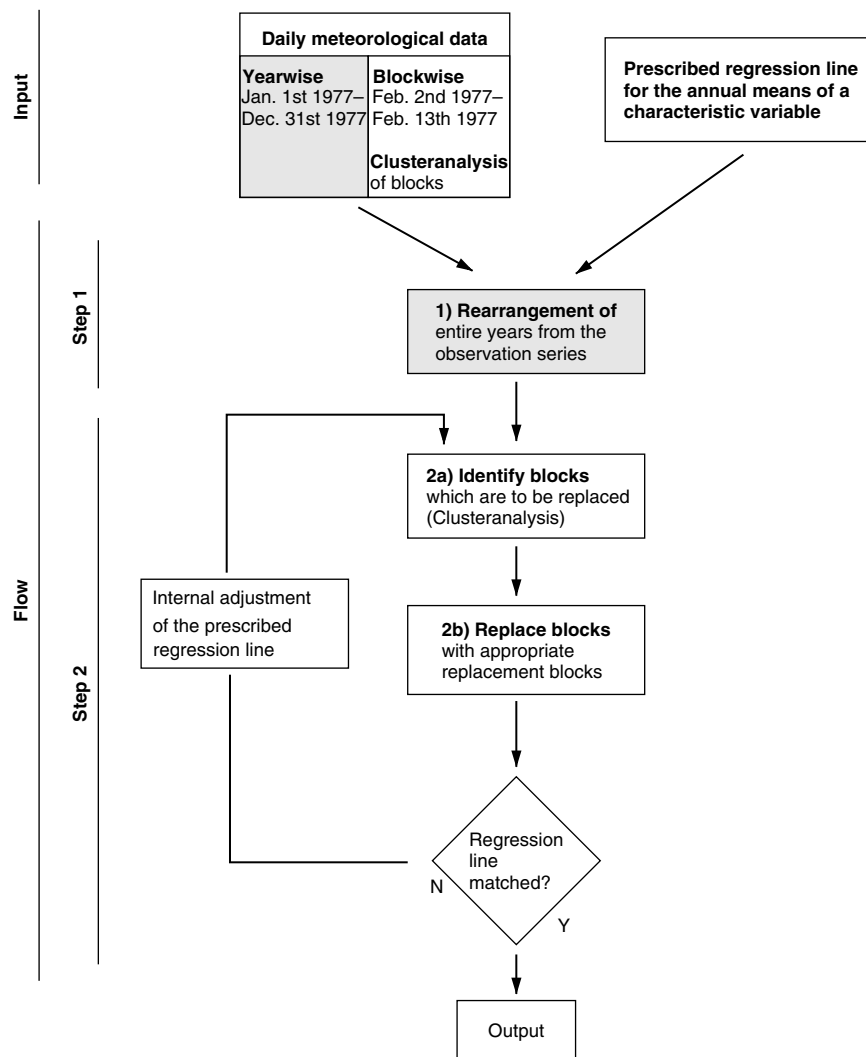


Figure 6. Summary of the generation of the date-to-date mapping.

mapping for this case. It comprises two steps operating at different time scales.

The first step operates on the time scale of years (parts of the flow chart concerned with this time scale are shaded in grey). It generates a first approximation to the mapping which consists of a simple rearrangement of entire calendar years from the training period. This rearrangement is chosen out of a large random sample of shuffled calendar years, such that its corresponding temperature series is as close as possible to the prescribed regression line. This series is guaranteed to exhibit realistic annual cycles and weather sequences within the single years, as they are simply copied from the observed series.

The second step alters this first approximation iteratively in order to find a series which matches the prescribed regression parameters exactly. This step replaces segments of 12 days length.

Replacing blocks instead of single days helps to obtain future series with realistic persistence, as the weather sequences within the blocks are again simply copied from the observed series. Experiments with station data from the region have shown that a block length of 12 days

essentially captures the persistence of the observed time series.

The blocks that are to be replaced are identified using a heuristic criterion based on a cluster analysis of the blocks, characterized by their 12 temperature observations (step 2 a in Figure 6). It decides, loosely speaking, whether any given block in the first approximation series contributes too much to the mismatch between the prescribed and the first approximation regression line.

The replacing blocks are selected from the blocks of the training period according to several heuristic rules (step 2 b). Besides temperature observations, these rules make use of the Julian days of the blocks, in order to select blocks from appropriate seasons. They define a set of potential replacements, which, firstly, brings the regression line of the resulting series closer to the prescribed one and, secondly, makes sure that the inserted replacement fits well into the parts of the series that have been set already. From this set of potential replacements, a block is chosen randomly. After the replacement of all 'bad' blocks, the date-to-date mapping is defined for the current iteration.

If despite these replacements the regression line of the future annual temperature means does not match the prescribed parameters (that is, the temperature mean and trend), this second step is iterated. Therefore, in order to compensate for a potential bias from the previous iteration, the next iteration is initialized by exaggerating the regression parameters (see Orłowsky *et al.*, 2008, for details).

Both at step 1 and at the end of step 2 b, years or 12-day blocks are drawn randomly. This makes any simulation a stochastic realization of the population of all possible simulations, which satisfy the prescribed regression parameters and the set of heuristic rules. The variety of the climate trajectories of this population can be estimated by analysing large ensembles of simulations.

Several locations: The approach is very similar to multi-location simulations (e.g. grid cells or stations), with the exception that it takes place in a parameter space of higher dimensionality. The ultimate goal, a date-to-date mapping, remains the same, which means that the series of future fields consist of spatial fields that were once observed during the training period.

In order to limit the dimensionality of the task, climatologically similar locations are classified in a preparatory step using cluster analysis (see the colour-coded clusters in Figure 1, and Section 2). For each of the clusters, linear regression parameters for the characteristic variable are prescribed, thereby allowing for the representation of spatially differentiated developments. Thus, ten numbers (e.g. five means and five linear trends) are prescribed to the RS scheme. All of them have to be reproduced by the RS within a certain tolerance which, for this application, is of up to 0.3 K (Table 2).

For this experiment, the temperature series within these spatial clusters are averaged over the respective grid cells, both for the training and the future periods. This yields one temperature series per period and cluster. From the averaged future-period series, annual means and their linear regression parameters are estimated. They give the parameters prescribed for the RS-scheme simulations. The averaged training-period series in turn constitutes the base for the entire construction of the date-to-date mapping: the selection of the permutation of entire years for the first approximation and of the subsequent identification of 'bad' blocks and their replacement is based on these averaged series merged together.

Appendix B

Cluster analysis is a classical tool for unsupervised pattern recognition from a set of observations (e.g. Steinhausen and Langer, 1977). For this work it is used (1) to identify the sub-regions of the RS-scheme area (Figure 1). They consist of similar grid cells, similar with respect to selected temperature statistics from the training period: mean temperature, standard deviation of temperature, and the difference between the mean of the second half and the mean of the first half of the

training period (that is, level, variability, and temporal development); (2) to identify circulation patterns from daily 500-hPa heights (Figure 2); (3) it is an important part of the RS scheme itself (see Orłowsky *et al.*, 2008).

For all three cases, a combination of hierarchical and non-hierarchical cluster analysis is used. Hierarchical methods, as opposed to their non-hierarchical relatives, do not operate on the observations themselves but on their mutual similarities or distances. Therefore the necessary distance matrix of the observations is calculated using the Euclidean distance. Cluster aggregation is based on the Minimal-Variance-distance, which tends to produce hyper-spherical clusters. A classification obtained thus is passed as initial classification to the non-hierarchical *k*-means algorithm (Hartigan and Wong, 1979).

In contrast to non-hierarchical methods, the results from a hierarchical classification do not depend on the initialization and the order in which the observations are processed. The initial classification it generates for the non-hierarchical part is therefore robust. The non-hierarchical part merely serves as a fine-tuning to achieve the unique representability of the clusters by their centres of mass, a mandatory feature for this application (see Section 2 and Orłowsky *et al.*, 2008), which cannot be guaranteed by means of a hierarchical cluster analysis alone.

The choice of the cluster number remains to a certain degree subjective. Both for the number of sub-regions and for the number of circulation patterns, it is based on visual inspection. Experiments with different cluster numbers have however not shown qualitatively differing results.

References

- Beersma J, Buishand T. 2003. Multi-site simulation of daily precipitation and temperature conditional on the atmospheric circulation. *Climate Research* **25**: 121–133.
- Briffa KR, Bartholin TS, Eckstein D, Jones PD, Karlen W, Schweingruber FH, Zetterberg P. 1990. A 1400-year tree-ring record of summer temperatures in Fennoscandia. *Nature* **346**: 434–439.
- Cassou C, Terray L, Hurrell JW, Deser C. 2004. North atlantic winter climate regimes: spatial asymmetry, stationarity with time, and oceanic forcing. *Journal of Climate* **17**: 1055–1068.
- Diez E, Primo C, Garcia-Moya J, Gutierrez J, Orfila B. 2005. Statistical and dynamical downscaling of precipitation over Spain from DEMETER seasonal forecasts. *Tellus* **57**: 409–423.
- Enke W, Spekat A. 1997. Downscaling climate model outputs into local and regional weather elements by classification and regression. *Climate Research* **8**: 195–207.
- Fraedrich K, Rückert B. 1998. Metric adaption for analog forecasting. *Physica A* **253**: 379–393.
- Hartigan JA, Wong MA. 1979. A K-means clustering algorithm. *Applied Statistics* **28**: 100–108.
- Jolliffe IT. 1990. Principal component analysis: a Beginner's guide - I. Introduction and application. *Weather* **45**: 375–383.
- Kageyama M, D'Andrea F, Ramstein G, Valdes PJ, Vautard R. 1999. Weather regimes in past climate atmospheric general circulation model simulations. *Climate Dynamics* **15**: 773–793.
- Kotlarski S, Block A, Böhm U, Jacob D, Keuler K, Knoche R, Rechid D, Walter A. 2005. Regional climate model simulations as input for hydrological applications: evaluation of uncertainties. *Advances in Geosciences* **5**: 119–125.
- Lorenz EN. 1969. Atmospheric predictability as revealed by naturally occurring analogues. *Journal of the Atmospheric Sciences* **26**: 636–646.

- Mann ME, Bradley RS, Hughes MK. 1998. Global-scale temperature patterns and climate forcing over the past six centuries. *Nature* **392**: 779–787.
- Marsland S, Haak H, Jungclaus J, Latif M, Röske F. 2003. The Max-Planck-Institute global ocean/sea ice model with orthogonal curvilinear coordinates. *Ocean Modelling* **5**: 91–127.
- Nakicenovic N, Swart R. 2001. *IPCC Special Report on Emissions Scenarios*. Cambridge University Press: Cambridge.
- Orlowsky B, Gerstengarbe FW, Werner PC. 2008. A resampling scheme for regional climate simulations and its performance compared to a dynamical RCM. *Theoretical and Applied Climatology* **92**: 209–223.
- Roeckner E. 2006. ENSEMBLES ECHAM5-MPI-OM SRESA1B run1, daily values, CERA-DB “ENSEMBLES_MPEH5_SRA1B_1_D”. http://cera-www.dkrz.de/WDCC/ui/Compact.jsp?acronym=ENSEMBLES_MPEH5_SRA%1B_1_D (March 1st 2007).
- Roeckner E, Bäuml G, Bonaventura L, Brokopf R, Esch M, Giorgetta M, Hagemann S, Kirchner I, Manzini LKE, Rhodin A, Schlese U, Schulzweida U, Tompkins A. 2003. The atmospheric general circulation model ECHAM 5, PART I: Model description. Technical Report. MPI-report No. 349. MPI for Meteorology, Hamburg.
- Sheather SJ, Jones M. 1991. A reliable data-based bandwidth selection method for kernel density estimation. *Journal of the Royal Statistical Society* **53**: 683–690.
- Solomon S, Qin D, Manning M, Marquis M, Averyt K, Tignor MMB, LeRoy H, Miller J, Chen Z. 2007. *Climate Change 2007, The Physical Science Basis. Contribution of Working Group I to the Fourth Assessment Report of the IPCC*. Cambridge University Press: Cambridge.
- Steinhausen D, Langer K. 1977. *Clusteranalyse - Einführung in Methoden und Verfahren der automatischen Klassifikation*. Walter de Gruyter: Berlin.
- Timbal B, McAvaney B. 2001. An analogue-based method to downscale surface air temperature: application for Australia. *Climate Dynamics* **17**: 947–963.
- Wang R, Wang S, Fraedrich K. 1991. An approach to reconstruction of temperature on a seasonal basis using historical documents from China. *International Journal of Climatology* **11**: 381–392.
- Wanner H, Brönnimann S, Casty C, Gyalistras D, Luterbacher J, Schmutz C, Stephenson DB, Xoplaki E. 2001. North Atlantic Oscillation: concepts and studies. *Surveys in Geophysics* **22**: 321–381.
- Werner P, Gerstengarbe FW. 1997. Proposal for the development of climate scenarios. *Climate Research* **8**: 171–182.
- Zorita E, von Storch H. 1999. The analog method as a simple statistical downscaling technique: comparison with more complicated methods. *Journal of Climate* **12**: 2474–2489.